Essential roles for Pot1b in HSC self-renewal and survival

Yang Wang,[1] Mei-Feng Shen,[1] and Sandy Chang[1]

[1]Department of Laboratory Medicine, Yale University School of Medicine, New Haven, CT

Maintenance of mammalian telomeres requires both the enzyme telomerase and shelterin, which protect telomeres from inappropriately activating DNA damage response checkpoints. Dyskeratosis congenita is an inherited BM failure syndrome disorder because of defects in telomere maintenance. We have previously shown that deletion of the shelterin component Pot1b in the setting of telomerase haploinsufficiency results in rapid telomere shortening and fatal BM failure in mice, eliciting phenotypes that strongly resemble human syskeratosis congenita. However, it was unclear why BM failure occurred in the setting of *Pot1b* deletion. In this study, we show that Pot1b plays an essential role in HSC survival. Deletion of *Pot1b* results in increased apoptosis, leading to severe depletion of the HSC reserve. BM from *Pot1b*$^{\Delta/\Delta}$ mice cannot compete with BM from wild-type mice to provide multilineage reconstitution, indicating that there is an intrinsic requirement for Pot1b the maintenance of HSC function in vivo. Elimination of the p53-dependent apoptotic function increased HSC survival and significantly extended the lifespan of *Pot1b*-null mice deficient in telomerase function. Our results document for the first time the essential role of a component of the shelterin complex in the maintenance of HSC and progenitor cell survival. (*Blood*. 2011;118(23): 6068-6077)

Introduction

Mammalian aging is associated with a functional decline in tissues that require continuous cellular renewal. Increasing evidence suggest that attenuation of stem cell functions could in part account for the proliferative defects observed in aging tissues. The acquisition of an unstable genome and the activation of p53-dependent DNA damage response pathways have been linked to stem cell degeneration during the aging process.[1] Telomeres, protein-DNA complexes that cap the ends of chromosomes, play important roles in preventing the activation of DNA damage checkpoints that induce cell-cycle arrest and apoptosis. Telomeres consist of G-rich simple repeat sequences that terminate in a single-stranded 3′ G-rich overhang. They are maintained by the enzyme telomerase, a specialized ribonucleoprotein complex that includes an RNA template (TERC) and a reverse transcriptase catalytic subunit (TERT).[2,3] Overexpression of telomerase in fibroblasts extends telomeres and prevents the onset of replicative senescence, indicating that telomerase is required for cellular immortalization.[3]

Although telomerase is specifically expressed in stem and progenitor cells, telomeres in highly proliferative tissues continue to shorten with increasing age. In the human hematopoietic system, progressive telomere shortening is observed in aging HSCs[4] and white blood cells.[5] Increasing evidence suggests that this critical telomere shortening results in stem cell failure, increased mortality, and increased incidence of cancer. Dyskeratosis congenita (DC) is a multisystem disorder characterized in patients by BM failure, skin abnormalities, and increased risk of cancer. Autosomal forms of this disease occur as the result of mutations in both components of telomerase, suggesting that telomerase mutations result in multisystem stem cell disorder.[6,7]

Disease anticipation, in which offsprings exhibit accelerated onset of disease phenotypes, is observed in patients with DC who are haploinsufficient for telomerase,[8,9] consistent with telomere shortening as a mechanism for anticipation. Dysfunctional telomeres also contribute to age-related disease processes in healthy elderly individuals, as an analysis of telomere lengths of individuals older than 60 years of age revealed that patients possessing shorter telomeres than age-matched control individuals had significantly poorer survival, attributed in part to an elevated mortality rate from heart and infectious diseases.[10] *mTerc*-null mice bearing dysfunctional telomeres display reduced proliferation of T and B lymphocytes, splenic atrophy with a reduction in germinal center function, and the absence of spermatogenesis and a decrease in the number of oocytes.[11,12] Of importance, reconstitution of telomerase activity in late-generation *mTerc*$^{-/-}$ and *mTert*$^{-/-}$ mice increased telomere lengths, reduced the level of DNA damage signaling, and rescued most of the pathologies associated with telomere dysfunction.[13] These results suggest that restoration of telomerase activity is able to eliminate the genotoxic stress caused by dysfunctional telomeres, restoring stem cell reserves and the functional status of highly proliferative organs.[14]

Besides telomerase, the proper maintenance of telomeres also require 6 telomere-specific binding proteins that form a complex, termed shelterin, which protects telomeres from inappropriately activating DNA damage response (DDR) checkpoints. Three sequence-specific DNA binding proteins are recruited to chromosomal ends: the duplex telomere binding proteins TRF1 and TRF2 and the single-stranded telomere DNA binding protein POT1. Adaptor proteins TIN2 and TPP1 link POT1 to TRF1/TRF2. POT1 homologs have been identified in all eukaryotes, and all POT1 proteins contain 2 highly conserved oligosaccharide-oligonucleotide folds to bind to the 3′ terminus of the single-stranded G-rich telomeric overhang.[15] Most vertebrates, including

Submitted June 16, 2011; accepted September 18, 2011. Prepublished online as *Blood* First Edition paper, September 23, 2011; DOI 10.1182/blood-2011-06-361527.

The online version of this article contains a data supplement.

The publication costs of this article were defrayed in part by page charge payment. Therefore, and solely to indicate this fact, this article is hereby marked "advertisement" in accordance with 18 USC section 1734.

humans, possess a single *POT1* gene, whereas the rodent genome encodes 2 *Pot1* genes, *Pot1a* and *Pot1b*.[16-18] Pot1a is an essential protein and functions to repress an ATR-dependent DDR at telomeres, whereas Pot1b protects the C-strand of telomeres from extensive nucleolytic degradation.[16,19,20] Deletion of *Pot1a* and *Pot1b* results in telomere dysfunction that engages a DDR, suggesting that proper capping of telomeres by both Pot1 proteins is critically important to protect telomeres from being recognized as damaged DNA.

Most of the known DC mutations have been found to affect core components of the telomerase holoenzyme. However, in recent studies, investigators have revealed that mutations in the shelterin component TIN2 result in a very severe form of DC. Patients with TIN2 mutations have very short telomeres, which culminate in premature failure of BM.[21,22] These data suggest that DC could also arise as a consequence of perturbation of components of the shelterin complex. We and others have previously shown that Pot1b deletion coupled with telomerase haploinsufficiency results in mice that display phenotypes strongly resembling human DC, including rapid telomere shortening, cutaneous syndromes, and fatal BM failure.[19,20] However, it was not known why BM failure occurred in this mouse model because BM failure was never observed in mice lacking telomerase[11,12] and was not apparent in 11-month-old *Pot1b*-null mice.[20]

In the current study, we uncover a critical role for Pot1b in maintaining HSC homeostasis. We show that Pot1b by itself, even in the setting of wild-type telomerase activity, is required for the survival of HSCs. In the absence of Pot1b, a DDR is activated at telomeres, resulting in the severe depletion of the HSC reserve via p53-dependent apoptosis. $Pot1b^{\Delta/\Delta}$ BM cells are unable to compete with BM isolated from wild-type mice to provide multilineage reconstitution, indicating that there is an intrinsic requirement for Pot1b in the maintenance of HSC function in vivo. The elimination of the p53-dependent apoptotic functions in *Pot1b*-null mice significantly extended the organismal lifespan, suggesting that Pot1b is required to repress a DDR at dysfunctional telomeres that would otherwise initiate p53-dependent apoptosis to inhibit HSCs proliferation. Our results therefore reveal a novel and essential role for Pot1b in the maintenance of HSC self-renewal capacity.

Methods

Mice

The generation of $Pot1b^{\Delta/\Delta}$, $p53^{R172P}$ and $mTerc^{-/-}$ mice were described previously.[11,20,23] ICR severe combined immunodeficiency (SCID) mice were purchased from The Jackson Laboratory. All mice were maintained according to Yale University Institutional Animal Care and Use Committee-approved protocols.

Isolation of total BM cells

For every animal, BM was isolated from the hind limb bones. The bones were dissected, and the marrow was flushed through a 21-gauge needle into $HBSS^+$ (Invitrogen), 2% FBS (Invitrogen), and 10mM HEPES. The cells were passed through 25-gauge needle twice and filtered (45-μm filter) to ensure single-cell suspension. Nucleated cells were counted manually after the lysis of RBCs with 3% acetic acid in methylene blue (StemCell Technologies).

5-Fluorouracil treatment

We used 5-fluorouracil (5-FU; 75 mg/kg intraperitoneally) for myelosuppression. Recovery of hematopoiesis was monitored by serial peripheral blood counts every 6 days for each mouse. Retro-orbital peripheral blood (< 50 μL per mouse) was obtained from anesthetized mice and collected into EDTA-coated capillary tubes for analysis.

Flow cytometry analysis

A total of 1×10^7 total BM cells was centrifuged and resuspended in 200 μL of $HBSS^+$. Cells were stained for 15 minutes with a cocktail of antibodies that included 9 lineage markers: Ter-119, CD3, CD4, CD8, B220, CD19, IL-7Rα, GR-1, and Mac-1 (eBioscience) conjugated to APC-Cy-7 (47-4317; eBioscience). In addition, the cocktail also contained anti–Sca-1-PE (12-5981; eBioscience) and anti–c-Kit-APC (17-1171; eBioscience). After staining, cells were washed, resuspended in $HBSS^+$, and analyzed by flow cytometry (Calibur or LSRII; BD Biosciences). LSK populations were selected on the basis of low or negative expression of the mature lineage markers and dual-positive expression for Sca-1 and c-Kit. To determine the proliferative status of LSK cells, BrdU was injected into mice (intraperitoneally) at the dosage of 150 mg/kg 2 hours before they were killed.

An analysis of BrdU incorporation was performed with the FITC BrdU flow kit (BD Biosciences). To quantitatively determine the percentage of cells that are actively undergoing apoptosis, BD Pharmingen's annexin V-PE Apoptosis Detection Kit was used. For cell-cycle parameters measured by Pyronin Y and Hoechst, BM cells were first stained for the lineage cell surface markers as well as Sca-1 and c-Kit antibodies. Cells were then resuspended in HBSS, 20mM HEPES, 1 g/L glucose, 10% FCS, and 1.7μM Hoechst 33342 and incubated for 1 hour at 37°C. After a single wash, BM cells were incubated in the same buffer containing Pyronin Y (1 μg/mL) for an additional hour at 37°C before analysis. FlowJo was used for all data analysis.

Competitive BM transplantation

Because our mouse cohorts are kept in a mixed genetic background, competitive BM transplantations were performed with the use of irradiated SCID recipients. Nucleated cells isolated from the BM were prepared as described previously, with male and female donor cells mixed together at a ratio of 1:1. A total of 1×10^7 mixed cells were injected retro-orbitally into 5.0-Gy–irradiated SCID recipient mice. Irradiated control mice that were not injected were used in every experiment, and these mice died within 10 days of treatment. To assess reconstitution, BM cells from recipient mice were analyzed by FISH with a Y-chromosome probe 3 months after transplantation. A minimum of 3 mice per genotype were used for reconstitution experiments.

Colony-forming assay and long-term culture-initiation cell assay

For short-term culture, 1×10^4 BM mononucleated cells were cultured in 35-mm dishes containing MethoCult 3434 (StemCell Technologies) following the manufacturer's protocols. Colonies were counted on day 12. For long-term culture-initiation cell assay assays, serial 2-fold dilutions were performed on initial isolates of 30 000 BM mononucleated cells/well; 12 replicates per BM were performed. After 4 weeks of weekly replenishment with MethoCult 5300 (StemCell Technologies), cells were trypsinized and plated on media MethoCult 3434 and cultured for 10 days before the percentage of negative wells per dilution was scored. Frequencies were calculated with the use of Poisson statistics (L-cal program from StemCell Technologies).

Microscopy

Metaphase chromosomes from BM were prepared 1-2 hours after treatment with colcemide, as previously described,[18] and subjected to Giemsa staining and/or telomere-peptide nucleic acid-FISH staining to label telomeres. Depending on the quality of metaphase spreads, 20-40 metaphases from each sample were analyzed in detail. FISH with a Y-probe was performed as previously described.[24] To quantitate dysfunctional telomeres in LSK cells, dysfunctional telomere-induced DNA damage foci (TIF) analysis was performed as previously described.[25]

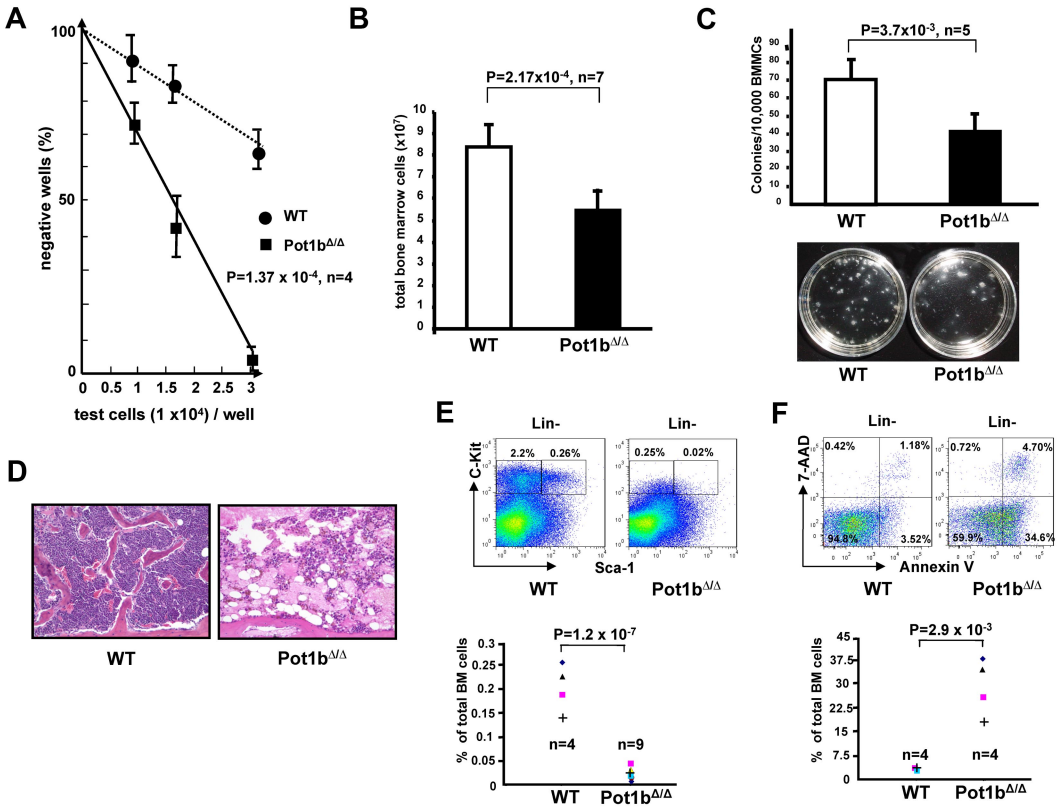

Figure 1. Defective hematopoiesis in *Pot1b*$^{\Delta/\Delta}$ mice. (A) The long-term culture-initiation cell assay was used to enumerate primitive BM progenitor cells in 2-month-old wild-type and *Pot1b*$^{\Delta/\Delta}$ mice (n = 4 mice per genotype, $P = 1.0 \times 10^{-4}$). (B) Numbers of total BM nucleated cells isolated from 6-month-old *Pot1b*$^{\Delta/\Delta}$ mice compared with age- and sex-matched wild-type controls (n = 7 mice per genotype, $P = 2.2 \times 10^{-4}$). Error bars represent SEM. (C) Numbers of colonies arising from 10^4 mono-nucleated wild-type (WT) and *Pot1b*$^{\Delta/\Delta}$ BM cells seeded in methylcellulose. Results are mean from 5 experiments ($P = 3.7 \times 10^{-3}$). Error bars represent SEM. Representative images were obtained after 12 days in culture. (D) BM morphology of bone diaphysis of a pair of a 15-month-old wild-type and *Pot1b*$^{\Delta/\Delta}$ mice (magnification ×20). (E) Expression of Sca-1 and c-Kit in multilineage-negative BM cells from wild-type (WT) and *Pot1b*$^{\Delta/\Delta}$ mice. Results were expressed as percentage of total nucleated BM cells for each fraction. The bottom panel shows data from 4 wild-type mice and 9 *Pot1b*$^{\Delta/\Delta}$ mice ($P = 1.2 \times 10^{-7}$). (F) Annexin V/7-AAD FACS profiles of BM derived from aged wild-type and *Pot1b*$^{\Delta/\Delta}$ mice. Bottom panel shows data from 4 wild-type and 4 *Pot1b*$^{\Delta/\Delta}$ mice ($P = 2.9 \times 10^{-3}$).

Reverse transcriptase–coupled real-time PCR

Total RNA was prepared by the use of the QIAGEN RNeasy Micro kit (no.740 04) according to manufacturer's instructions. For first-strand cDNA synthesis, 1 μg of total RNA, 20 pmol of Oligo(dT)12-18, and 200 units of SuperScript II Reverse transcriptase (Invitrogen) were mixed in a final volume of 20 μL. Then, 1 μL of synthesized cDNA was added to 20 μL of PCR mixture containing 1 × TaqMan Gene Expression Assay primers (Applied Biosystems) and 1 × TaqMan Universal PCR Master Mix (4324018; Applied Biosystems). Each sample was amplified in triplicate. PCR consisted of 40 cycles of denaturation at 95°C for 15 seconds and annealing and amplification at 60°C for 60 seconds in an ABI7900HT Sequence Detection System Machine (Applied Biosystems). The specific primers for TaqMan Gene Expression Assay primers were *PUMA*: Mm00519268_m1; *Bax*: Mm00432050_m1; and *p21*: Mm00432448_ml. 18S rRNA primers (4319413E) were used as internal control.

Results

Loss of *Pot1b* provokes proliferative defects in HSCs

The role of the shelterin component Pot1b in HSC function has not been previously addressed. Although deletion of *Pot1b* resulted in minimal impact on BM cellularity in 2-month-old *Pot1b*$^{\Delta/\Delta}$ mice (8.22×10^7 wild-type cells vs 7.5×10^7 *Pot1b*$^{\Delta/\Delta}$ cells, $P = .30$; supplemental Figure 1, available on the *Blood* Web site; see the Supplemental Materials link at the top of the online article), a significant decrease in the proliferative capacity of primitive progenitors was revealed in these mice by long-term culture-initiation cell assays (Figure 1A). By 6 months of age, the total BM nucleated cells count in all *Pot1b*$^{\Delta/\Delta}$ mice was significantly decreased compared with those from age-matched wild-type control mice (8.39×10^7 for wild-type vs 5.44×10^7 for *Pot1b*$^{\Delta/\Delta}$ BM; $P = 2.2 \times 10^{-4}$, n = 7; Figure 1B). These *Pot1b*-null BM cells also formed fewer colonies in an in vitro colony-forming assay (68 ± 13 CFUs for wild-type vs 45 ± 8 for *Pot1b*$^{\Delta/\Delta}$ BM; $P = 3.7 \times 10^{-3}$, n = 5), demonstrating a defect in the proliferation of myeloid progenitor cells (Figure 1C).

By 15 months of age, leucopenia, anemia and thrombocytopenia were readily apparent in the peripheral blood of *Pot1b*-null mice (supplemental Figure 2). BM hypocellularity was also readily detected in the femurs of these mice (Figure 1D), suggesting that the defect in BM proliferation might be because of progressive loss of the HSC population. To investigate this possibility, we examined the number of LSK (Lin^-, $Sca\text{-}1^+$, $c\text{-}kit^+$) cells, a population enriched in HSCs and multipotent progenitors (hematopoietic progenitor cells), and Lin^- $Sca\text{-}1^-$ $c\text{-}Kit^+$ (LK) cells, a population enriched in hematopoietic progenitor cells, in 15-month-old *Pot1b*$^{\Delta/\Delta}$ mice and age-matched wild-type controls. FACS analysis revealed that both LSK (0.26% in wild-type controls vs 0.02% in *Pot1b*$^{\Delta/\Delta}$ mice) and LK (2.2% vs 0.25%) populations were profoundly depleted in *Pot1b*$^{\Delta/\Delta}$ mice (Figure 1E). 7-Aminoactinomycin (7-AAD)/annexin V staining revealed that both the BM and the peripheral blood of 15-month-old *Pot1b*$^{\Delta/\Delta}$ mice displayed a 9-fold

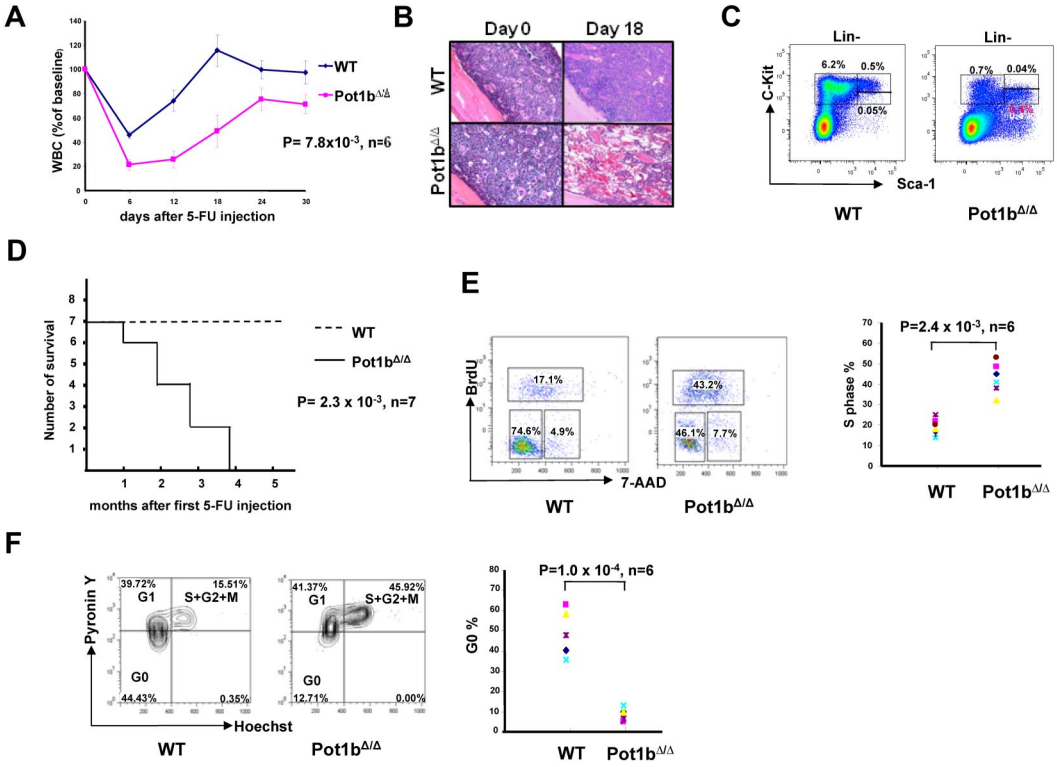

Figure 2. HSC exhaustion in the absence of Pot1b. (A) Serial peripheral blood count was used to monitor 2-month-old wild-type (WT) and *Pot1b*$^{\Delta/\Delta}$ mice injected with a single dose of 5-FU (75 mg/kg, intraperitoneally). WBC counts are shown as a percentage of the initial baseline values for each group of mice (n = 6 mice per genotype, $P = 7.8 \times 10^{-3}$). Error bars represent SEM. (B) BM morphology (magnification ×20) before and 18 days after 5-FU injection for wild-type (WT) and *Pot1b*$^{\Delta/\Delta}$ mice. (C) Representative FACs analysis of multilineage negative cells 12 days after 5-FU injection. Results are expressed as percentage of total nucleated BM cells for each fraction. (D) Survival outcome of sequentially 5-FU–injected wild-type (WT) and *Pot1b*$^{\Delta/\Delta}$ mice. Results were analyzed with a log-rank nonparametric test and expressed as Kaplan-Meier survival curves (n = 7 mice per genotype, $P = 2.3 \times 10^{-3}$). (E) Representative cell-cycle analysis on LSK cells isolated from both wild-type (WT) and *Pot1b*$^{\Delta/\Delta}$ mice. Data from the 6 experiments are shown in the right panel ($P = 2.4 \times 10^{-3}$). (F) LSK cells were stained for DNA (Hoechst 33 342) and RNA (Pyronin Y) to assess the relative proportions in the G_0, G_1 phases of the cell cycle. Data from 6 experiments are shown in the right panel ($P = 1.0 \times 10^{-4}$).

increase in the number of apoptotic cells compared with age-matched wild-type controls (BM: 34.6% vs 3.52%, $P = 2.9 \times 10^{-3}$; PB: 54.6% vs 6.5%, $P = 1.6 \times 10^{-3}$; Figure 1F, supplemental Figure 3), suggesting that an increase in apoptosis in the absence of Pot1b directly contributes to the proliferative defects observed in HSCs. Taken together, these results suggest that Pot1b plays a critically important role in maintaining HSC proliferation.

HSC exhaustion in the absence of Pot1b

The LSK HSCs in wild-type mice exist predominantly in a quiescent, Ki67-negative state[26] and are resistant to the antiproliferative agent 5-FU. Wild-type mice survive repeated treatments with 5-FU because dormant, drug-resistant HSCs can be induced to cycle, rapidly generating new cells to replenish depleted reserves. Proliferating HSCs, however, are extremely sensitive to 5-FU. We hypothesize that because of homeostatic response to the depletion of HSCs in the BM, the LSK population is likely actively cycling in Pot1b null mice, resulting in exhaustion of stem cell function.

To test this hypothesis, we administered a single dose of 5-FU to both 2-month-old wild-type and *Pot1b*$^{\Delta/\Delta}$ mice and performed serial peripheral bleeds to monitor for leucopenia. Compared with wild-type controls, severe leucopenia, followed by a delayed recovery in leukocyte numbers, was observed in 5-FU treated *Pot1b*$^{\Delta/\Delta}$ mice (Figure 2A). Whereas BM from wild-type mice exhibited hyperproliferation 18 days after the administration of 5-FU, BM of 5-FU treated *Pot1b*$^{\Delta/\Delta}$ mice remained markedly hypocellular (Figure 2B). Examination by FACS analysis of the LK population 12 days after treatment with 5-FU revealed that BM derived from wild-type mice possessed almost 9 times more LK cells than BM isolated from *Pot1b*$^{\Delta/\Delta}$ mice (6.2% vs 0.7%; Figure 2C). Although the total number of LSK cells appear similar between wild-type and *Pot1b*$^{\Delta/\Delta}$ mice (0.55% vs 0.44%), it is important to note that in wild-type mice most of the LSK cells are c-Kit^{high} (0.5%), whereas those in *Pot1b*$^{\Delta/\Delta}$ mice are c-Kit^{low} (0.4%; Figure 2C). It has been shown that the c-Kit^{high} fraction of LSK cells includes long-term repopulation HSCs and that the c-Kit^{low} fraction does not have this repopulation capacity.[27] To further investigate the consequences of hematopoietic defects in *Pot1b*$^{\Delta/\Delta}$ mice, monthly 5-FU injections were administered to 2-month-old wild-type and *Pot1b*$^{\Delta/\Delta}$ mice. After 4 cycles of 5-FU treatment, 100% of *Pot1b*$^{\Delta/\Delta}$ mice died, whereas all wild-type mice survived ($P = 2.3 \times 10^{-3}$, n = 7; Figure 2D).

To test the hypothesis that LSK cells derived from *Pot1b*$^{\Delta/\Delta}$ mice are actively cycling, in vivo BrdU injections were performed to label hematopoietic cells. The percentage of LSK cells in S phase was significantly greater in *Pot1b*$^{\Delta/\Delta}$ cells compared with wild-type control mice ($P = 2.4 \times 10^{-3}$, n = 6; Figure 2E). To determine whether BrdU incorporation in *Pot1b*$^{\Delta/\Delta}$ LSK cells correlated with a decrease in the quiescent G_0 LSK population, we used a combination of DNA (Hoechest 33342) and RNA (Pyronin Y) staining to distinguish between the G_0 and G_1 cell populations. A significant reduction in quiescence was observed in *Pot1b*$^{\Delta/\Delta}$ LSK cells. In wild-type mice, 44.4% of LSK cells were quiescent (Hoechest and Pyronin Y double-negative) compared with 12.7% in *Pot1b*$^{\Delta/\Delta}$ cells ($P = 1.0 \times 10^{-4}$, n = 6; Figure 2F). Taken together, these results suggest that in the absence of Pot1b, HSCs

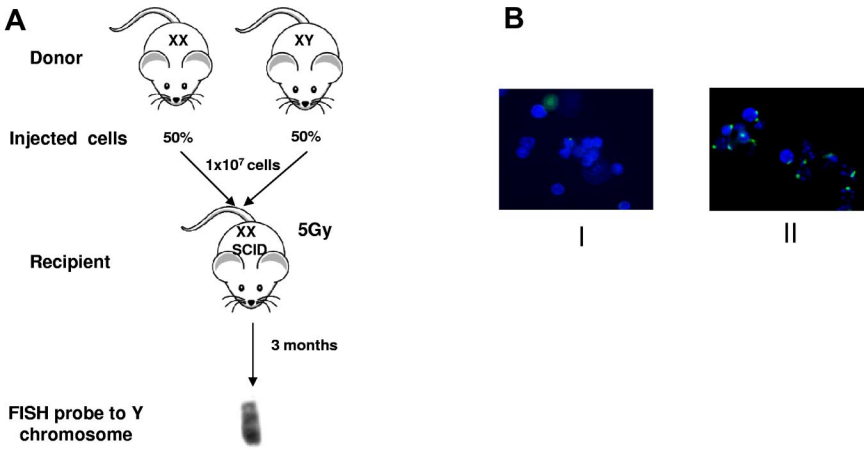

Figure 3. Intrinsic defect in *Pot1b*$^{\Delta/\Delta}$ mice hematopoietic cells. (A) Scheme of competitive BM transplantation experiment. Two-month-old male and female wild-type or *Pot1b*$^{\Delta/\Delta}$ mice were used as marrow donors. Female SCID recipient mice were lethally irradiated with 5 Gy of radiation. A total of 10 million mixed nucleated cells (50% from each genotype) were injected intravenously into the lateral tail veins of recipient mice. Recipients were killed after 3 months, and BM cells were analyzed with FISH for the presence of Y chromosomes. (B) Representative images of Y-probe FISH results in 2 different study groups. Group I: male *Pot1b*$^{\Delta/\Delta}$ male donors, wild-type female donors. Group II: wild-type male donors, *Pot1b*$^{\Delta/\Delta}$ female donors. Green: FITC labeled Y-FISH probe; blue: DAPI nuclear staining.

actively proliferate and are extremely sensitive to the presence of 5-FU. The delayed recovery in both peripheral blood count and BM cells after the administration of 5-FU is likely due to acute depletion of HSCs, resulting in defective stem cell renewal capacity, BM exhaustion, and early death.

An intrinsic requirement for Pot1b in the maintenance of HSC survival in vivo.

Because the deletion of *Pot1b* removes this protein from all cell types in the mouse, it is important to determine whether Pot1b plays a cell autonomous role in hematopoiesis. To address this question, we performed 1:1 competitive BM transplantation, in which male *Pot1b*$^{\Delta/\Delta}$ donor BM was mixed with age-matched female wild-type BM and then injected into lethally irradiated SCID mice. The converse experiment, in which male wild-type BMs were mixed with female *Pot1b*$^{\Delta/\Delta}$ donor BMs, also was performed. SCID mice were used as recipients for transplantation experiments because our mouse cohorts were maintained in a mixed genetic background. Three months after stable BM transplantation, FISH was used to quantify the number of the Y chromosomes present in cells prepared from the reconstituted BM. In 100% of experiments, BM from wild-type donors irrespective of sex always out competed BMs derived from *Pot1b*$^{\Delta/\Delta}$ mice (Figure 3; Table 1). These results indicate that there is an absolute and intrinsic requirement for Pot1b in the maintenance of HSC survival in vivo that cannot be attributed to stromal defects.

Elevated DNA damage response, chromosomal fusions, and apoptosis in HSCs devoid of Pot1b

Studies in human and mouse cell cultures and organ systems have shown that dysfunctional telomeres can engage classic DDR pathways.[28] There is now strong evidence that global activation of the DNA damage machinery by dysfunctional telomeres throughout proliferating cellular compartments initiates cellular checkpoint responses, which in turn lead to defects in cellular proliferation.[29,30] To test the hypothesis that dysfunctional telomeres activate the DDR in LSK cells devoid of Pot1b, we used the TIF assay to quantitatively determine the association of DNA damage proteins to dysfunctional telomeres.[31,32]

As expected, the DNA damage protein γ-H2AX did not associate with telomeres in wild-type LSK cells, with no wild-type cells displaying > 3 TIFs. In contrast, *Pot1b* deletion resulted in the dramatic induction of a DDR in LSK cells, with at least 3 TIFs observed in 38% ± 10% of *Pot1b*$^{\Delta/\Delta}$ BM cells examined (Figure 4A-B). Deletion of *Pot1b* also resulted in elevated p53 levels and the phosphorylation of Chk2 in BM multilineage negative cells, suggesting that the ATR-dependent DDR is activated in a cell population enriched with HSCs on *Pot1b* deletion (supplemental Figure 4). BM cells isolated from *Pot1b*$^{\Delta/\Delta}$ mice also displayed chromosomes with telomere-free ends and end-to-end chromosome fusions that increased with age, both hallmarks of severe telomere dysfunction (Table 2; Figure 4C-D).

We hypothesized that dysfunctional telomeres activate a DDR that initiates p53-dependent apoptosis and/or cellular senescence pathways, resulting in impaired HSC renewal and function. To test this hypothesis, we used real-time PCR analysis to monitor for the expression of downstream genes involved in p53-dependent apoptosis, including PUMA and Bax. *Pot1b*$^{\Delta/\Delta}$ LSK cells displayed a 4.2 ± 1.3-fold increase in *PUMA* expression ($P = 7.0 \times 10^{-3}$) and a 2.1 ± 0.64-fold increase in *BAX* expression ($P = 2.0 \times 10^{-2}$; Figure 4E). Consistent with these gene expression changes, 7-AAD/annexin V staining revealed that *Pot1b*$^{\Delta/\Delta}$ LSK cells exhibited consistently increased apoptosis (22.5% vs 7.8%, $P = 2.0 \times 10^{-4}$, n = 6; Figure 4F). Because telomere dysfunction can also induce the onset of cellular senescence in highly proliferative compartments,[30] we examined the expression level of *p21* in *Pot1b*$^{\Delta/\Delta}$ LSK cells. p21 plays a critical role in mediating p53-dependent cellular senescence.[33-35] However, compared with wild-type controls, no significant change in *p21* expression was detected in LSK cells devoid of Pot1b ($P = .36$; Figure 4E). Collectively, these results suggest that Pot1b plays a critical role in HSC telomere end protection, preventing the activation of a p53-dependent DDR at telomeres that would otherwise result in the initiation of an apoptotic response in HSCs.

Table 1. Summary of competitive BMT with BM nucleated cells from WT and *Pot1b*$^{\Delta/\Delta}$ mice

Study groups	I	II
Male donor genotype	*Pot1b*$^{\Delta/\Delta}$	WT
Female donor genotype	WT	*Pot1b*$^{\Delta/\Delta}$
Results: Y chromsome % in recipients	0, 0, 2.8, 3.1	90, 91, 93, 86

BMT indicates BM transplantation; and WT, wild-type.

Depletion of hematopoietic stem cells in *Pot1b*$^{\Delta/\Delta}$*; mTerc*$^{+/-}$ mice precedes BM failure

Pot1b is thought to protect the C-strand of telomeres from nucleolytic degradation, because mice lacking Pot1b have short

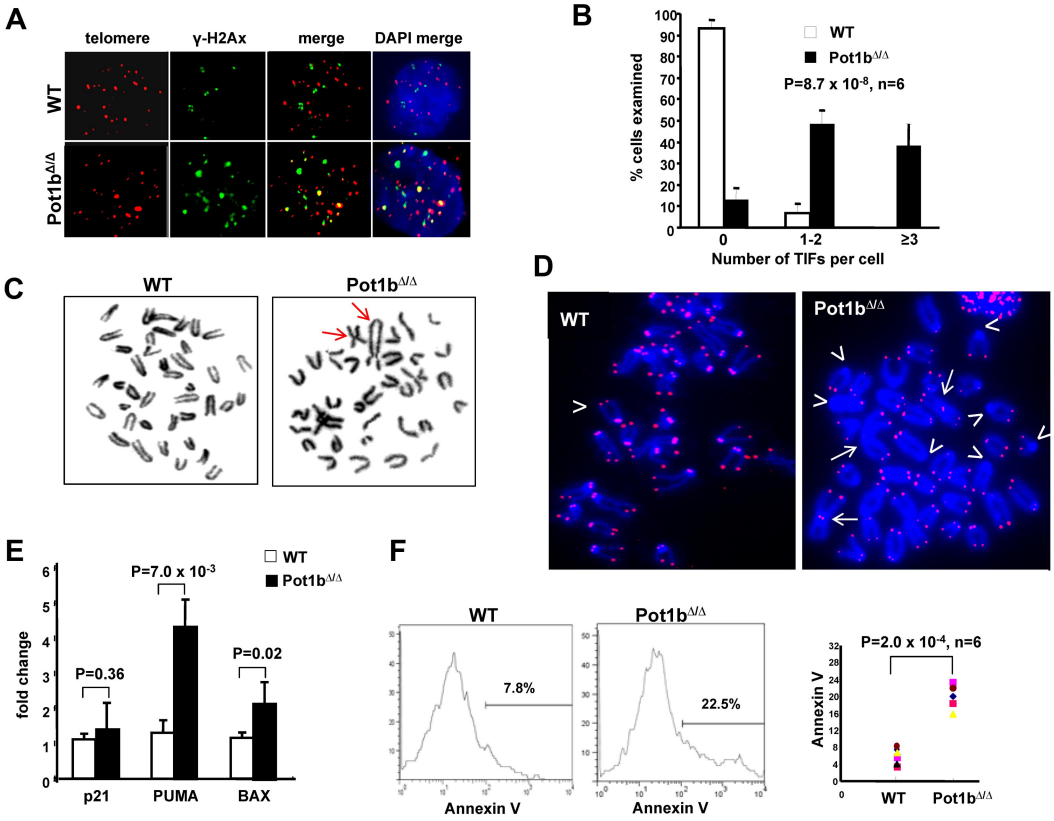

Figure 4. Elevated DNA damage response in HSCs lacking *Pot1b*. (A) Colocalization of γ-H2Ax (green) and TRF1 (red) to telomeres in sorted LSK cells isolated from wild-type (WT) and *Pot1b*$^{\Delta/\Delta}$ mice. Six 4-month-old mice per genotype were used for this experiment. (B) Quantification of colocalization of γ-H2Ax and TRF1 to telomeres in wild-type (WT) and *Pot1b*$^{\Delta/\Delta}$ LSK cells. A total of 300 nuclei were scored per genotype. Error bars represent SEM. (C) BM metaphases isolated from *Pot1b*$^{\Delta/\Delta}$ BM show chromosome end-to-end fusions (arrows), whereas wild-type (WT) metaphases show minimal abnormalities. (D) End-to-end chromosome fusions (arrows) and telomere signal-free ends (arrowheads) are elevated in *Pot1b*$^{\Delta/\Delta}$ BM cells. Not all telomere-free chromosome ends are indicated. (E) Representative real-time PCR quantification of mRNA expression levels of *p21*, *PUMA*, and *BAX* in sorted wild-type (WT) and *Pot1b*$^{\Delta/\Delta}$ LSK cells is shown. Each experiment was repeated in triplicate. Error bars represent SEM. (F) Histograms showing annexin V profiles of mice bone marrow LSK cells isolated from wild-type (WT) and *Pot1b*$^{\Delta/\Delta}$. Data from 6 mice per genotype are shown in the right panel ($P = 2.0 \times 10^{-4}$).

telomeres but very long 3′ G-overhangs.[16,19,20] Our data suggest that the HSCs of mice lacking Pot1b possess dysfunctional telomeres, resulting in profound defects in BM proliferation. In contrast, aberrations in the hematopoietic system are not readily observable even in late-generation telomerase knockout mice, suggesting that Pot1b loss impacts upon HSC proliferative functions more severely than deletion of telomerase. Because telomerase is essential for telomere elongation, we hypothesized that deletion of both *Pot1b* and telomerase will result in accelerated telomere shortening, leading to rapid HSC proliferative decline and complete BM failure at an early age.

Indeed, the *Pot1b*$^{\Delta/\Delta}$ mice heterozygous for telomerase (*mTerc*$^{+/-}$) experience accelerated telomere shortening and develop complete BM failure as early as 6 months of age.[20] However, it was not clear mechanistically why BM failure occurred in this setting. To understand the impact of accelerated telomere shortening on the HSC compartment, we examined LK, LSK cells, and BM cells derived from wild-type and *Pot1b*$^{\Delta/\Delta}$; *mTerc*$^{+/-}$ mice during a period of 6 months. Compared with wild-type mice at 2 months of age, a dramatic decrease in the number of LSK and LK cells were observed in *Pot1b*$^{\Delta/\Delta}$; *mTerc*$^{+/-}$ mice (LSK, 0.28% vs 0.12%; LK, 2.04% vs 1.04%; Figure 5A; supplemental Figure 5).

Although at this early age the BM still appeared relatively normal in vivo (Figure 5B), a reduction in the number of total BM cells was observed ($7.4 \pm 1.3 \times 10^7$ for wild-type vs $5.3 \pm 0.7 \times 10^7$ for *Pot1b*$^{\Delta/\Delta}$; *mTerc*$^{+/-}$ BM; Figure 5C). At 4 months of age, the frequency of the LSK population in *Pot1b*$^{\Delta/\Delta}$;*mTerc*$^{+/-}$ mice was reduced ~ 8-fold compared with wild-type controls (0.25% vs 0.03%), whereas the LK population was reduced ~ 4.5-fold (1.75% vs 0.39%; Figure 5A; supplemental Figure 5). This time point was also characterized by the appearance of a hypocellular BM (Figure 5B) and a 5-fold decrease in total BM cells ($8.2 \pm 1.2 \times 10^7$ vs $1.6 \pm 0.2 \times 10^7$, Figure 5C). By 6 months of age, LSK and LK cells were completely absent in *Pot1b*$^{\Delta/\Delta}$;*mTerc*$^{+/-}$ mice, and only ~ 2.5×10^6 nucleated cells were found in their BM (Figure 5A-C; supplemental Figure 5). These results suggest that the BM failure phenotype observed in 6-month-old *Pot1b*$^{\Delta/\Delta}$; *mTerc*$^{+/-}$ mice is because of progressive loss of the HSC population.

Table 2. Chromosome fusions in *Pot1b*$^{\Delta/\Delta}$ mice

Mouse	Sex	Age, mo	Meta-analyzed	Fusion/meta
4172	F	2	32	0
4314	M	2	32	0.03
8363	F	10	35	0.2
8367	F	12	34	0.8
7312	M	14	33	0.57
7245	F	14	33	1.1
6590	M	16	33	2.4
2510	M	16	34	2.0

F indicates female; M, male; and meta, metaphases.

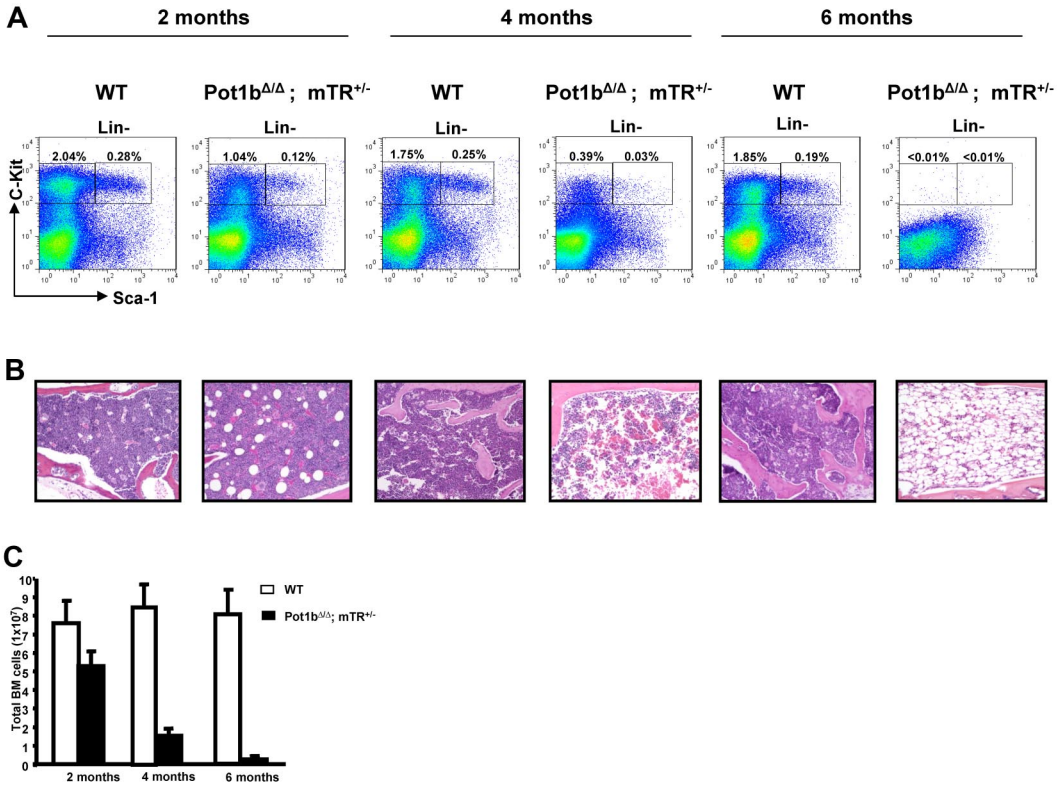

Figure 5. HSC exhaustion in *Pot1b*$^{\Delta/\Delta}$;*mTerc*$^{+/-}$ mice precedes BM failure. (A) FACs analysis of multilineage negative population in aging *Pot1b*$^{\Delta/\Delta}$; *mTerc*$^{+/-}$ mice. Numbers are the percentage of LSK and LK cells in total BM. Each age group represents a minimum of 4 mice. Lin−: muiltilineage negative. (B) BM morphology in the diaphysis of the bone of wild-type and *Pot1b*$^{\Delta/\Delta}$; *mTerc*$^{+/-}$ mice at the indicated ages (×20 magnification). Each image corresponds to the above flow cytometric analysis. (C) Quantification of total BM nucleated cell counts for wild-type (WT) and *Pot1b*$^{\Delta/\Delta}$; *mTerc*$^{+/-}$ mice at the indicated ages. Each age group represents a minimum of 4 mice. Error bars represent SEM.

Reduction of p53-dependent apoptotic function rescues the proliferative defects observed in *Pot1b*$^{\Delta/\Delta}$; *mTerc*$^{+/-}$ HSCs

The activation of p53-dependent genes involved in the apoptotic pathway, and the markedly elevated number of apoptotic HSCs observed in *Pot1b*$^{\Delta/\Delta}$ mice, suggested that increased apoptosis because of the activation of the p53 DDR pathway by dysfunctional telomeres was responsible for the depletion of HSCs. We therefore reasoned that abrogation of the apoptotic function of p53 will result in at least partial rescue of HSC proliferative capacity. To test this hypothesis, we used the *p53*$^{R172P/R172P}$ knock-in mouse (abbreviated as *p53*$^{P/P}$).[23] This point mutation substitutes the wild-type *p53* alleles with mutant *p53*, in which arginine at position 172 is replaced with proline. p53^{R172P} is the ortholog of a human p53 mutant that is completely defective for apoptosis but still able to mediate cellular senescence/cell cycle arrest.[23,30] By using the 1:1 competitive BM transplantation assay, we compared the ability of *Pot1b*$^{\Delta/\Delta}$; *p53*$^{P/P}$ BM cells versus *Pot1b*$^{\Delta/\Delta}$; *p53*$^{+/+}$ BM cells to reconstitute lethally irradiated SCID mice.

Three months after stable engraftment, we found that 75%-85% of engrafted BM cells originated from *Pot1b*$^{\Delta/\Delta}$; *p53*$^{P/P}$ donors (Table 3). These results indicate that *Pot1b*$^{\Delta/\Delta}$; *p53*$^{p/p}$ BM cells are able to out compete *Pot1b*$^{\Delta/\Delta}$; *p53*$^{+/+}$ BM cells to multilineage reconstitute lethally irradiated mice, most likely because of abrogation of the apoptotic function of p53 to enhance cellular survival and increased HSC proliferative capacity. Indeed, compared with age-matched *Pot1b*$^{\Delta/\Delta}$; *mTerc*$^{+/-}$; *p53*$^{+/+}$ mice, *Pot1b*$^{\Delta/\Delta}$; *mTerc*$^{+/-}$; *p53*$^{P/P}$ mice displayed increased numbers of LSK (0.08% vs 0.03%) and LK (0.75% vs 0.18%) cells, and a more robust trilineage BM that yielded 4-fold more colonies in an in vitro colony-forming assay (35 ± 8 vs 9 ± 5, $P = 9.6 \times 10^{-3}$, n = 3; Figure 6A-D). Taken together, these results suggest that elimination of the p53 apoptotic function in the setting of severe telomere dysfunction improved the proliferative capacity of HSCs.

Finally, we examined the overall survival rate of our mouse cohorts. The median survival of *Pot1b*$^{\Delta/\Delta}$; *mTerc*$^{+/-}$; *p53*$^{P/P}$ mice was significantly longer than that of *Pot1b*$^{\Delta/\Delta}$; *mTerc*$^{+/-}$; *p53*$^{+/+}$ mice (210 days vs 135 days, $P = 1.5 \times 10^{-2}$). *Pot1b*$^{\Delta/\Delta}$; *mTerc*$^{-/-}$; *p53*$^{P/P}$ mice also lived significantly longer than *Pot1b*$^{\Delta/\Delta}$; *mTerc*$^{-/-}$; *p53*$^{+/+}$ mice (33.5 days vs 17.5 days, $P = 1.8 \times 10^{-3}$; Figure 6E). These results suggest that abrogation of the p53-dependent apoptotic response significantly increased the lifespan of *Pot1b*$^{\Delta/\Delta}$; *mTerc*$^{+/-}$ and *Pot1b*$^{\Delta/\Delta}$; *mTerc*$^{-/-}$ mice by promoting HSC survival. However, compared with wild-type and *p53*$^{P/P}$ controls, *Pot1b*$^{\Delta/\Delta}$;*mTerc*$^{-/-}$; *p53*$^{P/P}$ mice still died earlier. This is most likely because of the fact that telomere dysfunction continues to persist in the setting of *Pot1b* deletion, as revealed by the elevated number of end-to-end chromosome fusions observed in the BM of *Pot1b*$^{\Delta/\Delta}$; *mTerc*$^{+/-}$; *p53*$^{P/P}$ mice (Table 4).

Table 3. Competitive BMT results for *Pot1b*$^{\Delta/\Delta}$ and *Pot1b*$^{\Delta/\Delta}$; *p53*$^{P/P}$ BM cells

Study groups	I	II
Male donor genotype	*Pot1b*$^{\Delta/\Delta}$	*Pot1b*$^{\Delta/\Delta}$; *p53*$^{P/P}$
Female donor genotype	*Pot1b*$^{\Delta/\Delta}$; *p53*$^{P/P}$	*Pot1b*$^{\Delta/\Delta}$
FISH results: chromosome Y% in each mouse	8, 6, 4	75, 84, 85

BMT indicates BM transplantation.

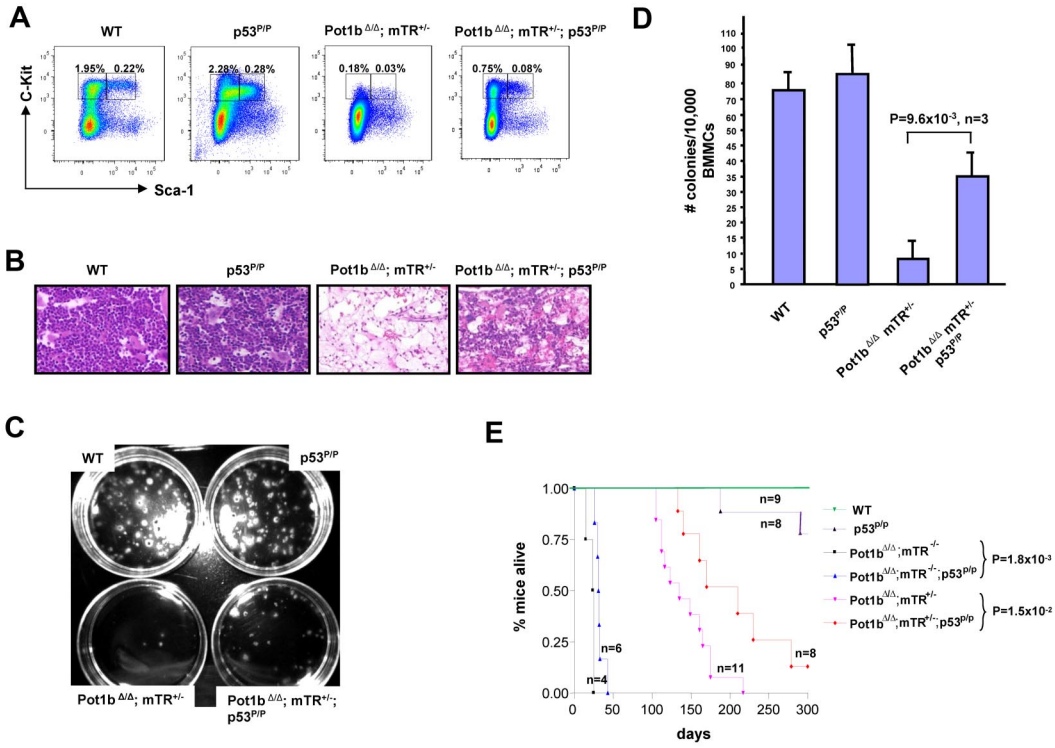

Figure 6. Abrogation of p53-dependent apoptotic function partially rescues the proliferative defects observed in *Pot1b*$^{\Delta/\Delta}$;*mTerc*$^{+/-}$ HSCs. (A) Frequency of LK and LSK cells isolated from age-matched wild-type, *p53*$^{P/P}$, *Pot1b*$^{\Delta/\Delta}$; *mTerc*$^{+/-}$, and *Pot1b*$^{\Delta/\Delta}$; *mTerc*$^{+/-}$; *p53*$^{P/P}$ BM. (B) BM morphology of age-matched wild-type (WT) *p53*$^{P/P}$, *Pot1b*$^{\Delta/\Delta}$; *mTerc*$^{+/-}$, and *Pot1b*$^{\Delta/\Delta}$; *mTerc*$^{+/-}$; *p53*$^{P/P}$ mice (×20 magnification) in the diaphysis of the bone. (C) Representative in vitro colony-forming assays of 10^4 BM mononucleated cells isolated from age-matched wild-type, *p53*$^{P/P}$, *Pot1b*$^{\Delta/\Delta}$; *mTerc*$^{+/-}$;*p53*$^{P/P}$, and *Pot1b*$^{\Delta/\Delta}$; *mTerc*$^{+/-}$ mice. (D) Quantification of the number of colonies shown in panel C. The average colony numbers for wild-type (WT) *p53*$^{P/P}$, *Pot1b*$^{\Delta/\Delta}$; *mTerc*$^{+/-}$, and *Pot1b*$^{\Delta/\Delta}$; *mTerc*$^{+/-}$; *p53*$^{P/P}$ mice are 73 ± 12, 84 ± 15, 9 ± 5, and 35 ± 8, respectively. Results are from 3 independent experiments. Error bars represent SEM. (E) Kaplan-Meier survival analysis of *Pot1b*$^{\Delta/\Delta}$; *mTerc*$^{+/-}$; *p53*$^{P/P}$ intercrosses and wild-type (WT), *p53*$^{P/P}$ mice as control. For clarity, not all genotypes generated are shown. *P* values are indicated for selected comparison groups.

Discussion

In this study, we show for the first time that the shelterin component Pot1b is critically important for the self-renewal function of HSC and progenitor cells. Pot1b is required for maintenance of HSC telomere stability because deletion of Pot1b results in the formation of dysfunctional telomeres that results in HSC proliferative defects. We show that there is an absolute and intrinsic requirement for Pot1b in the maintenance of HSC survival because BM cells from *Pot1b*$^{\Delta/\Delta}$ mice cannot compete with wild-type BM to long term reconstitute lethally irradiated recipients. In the absence of Pot1b, dysfunctional telomeres activate a p53-dependent DDR in HSCs, initiating a p53-dependent apoptotic response that ultimately results in a progressive decrease in the number of HSCs. Removal of Pot1b in the setting of telomerase haploinsufficiency accelerated telomere erosion, resulting in the rapid depletion of HSCs and complete BM failure in vivo. Finally, when the p53-dependent apoptotic response was genetically abrogated in vivo in the setting of both *Pot1b* deletion and telomerase haploinsufficiency, HSC proliferative defect was markedly reduced, resulting in a significant extension of organismal lifespan. Our results document mechanistically for the first time that p53-dependent apoptotic response is primarily responsible for compromised HSC self-renewal function when *Pot1b* is deleted in mice.

Table 4. Chromosome fusions in *Pot1b*$^{\Delta/\Delta}$; *mTerc*$^{+/-}$; *p53*$^{p/p}$ cells

Mouse	No. of meta analyzed	Meta with fusions, %	Fusion/meta
6767	32	100	4.9
5998	35	65.7	2.6
6850	33	100	7.2
7035	34	97	3.9

Meta indicates metaphase.

Defects in telomere maintenance contribute directly to a spectrum of acquired and inherited human hematopoietic disorders.[36-39] Shortened telomeres and mutations in *TERC* and *TERT* are present in BM failure syndromes, including aplastic anemia, myelodysplastic syndrome, and DC.[40,41] Recently, mutations in the shelterin component TIN2 have been identified in DC patients who do not possess mutations in the genes encoding components of the telomerase complex.[21,22] The prevalence for these mutations has been estimated to be as high as 11% of all DC patients.[22] Another shelterin component, TPP1, is required to recruit telomerase to telomeres,[42,43] and this recruitment is augmented by TPP1's interaction with TIN2.[44,45] Of importance, telomerase recruitment is disrupted by TIN2 DC mutations.[44]

These results suggest that DC could arise not only from defects in telomerase function per se but through the failure of telomerase to properly localize to and repair dysfunctional telomeres due to mutations in components of the shelterin complex. The results presented here present additional evidence for the importance of the shelterin complex in maintaining hematopoietic function. Proliferative defects in BM arise even in the setting of fully functional telomerase when Pot1b function is compromised. A particularly important question is why deletion of *Pot1b* resulted in proliferative BM defects, whereas late-generation *mTerc*$^{-/-}$ mice lacking telomerase activity bearing critically shortened telomeres

do not display this phenotype.[46] When *Pot1b* is deleted in mice in the setting of telomerase haploinsufficiency, accelerated telomere shortening is accompanied by phenotypes characteristic of human DC, including cutaneous phenotypes and fatal BM failure.[19,20] The $Pot1b^{\Delta/\Delta}$; $mTerc^{+/-}$ mouse thus represents a useful model to understand the roles of shelterin components and telomerase in the maintenance of HSC telomeres, observations that will likely shed light on the pathogenesis of BM failure syndromes.

Most vertebrates, including humans, possess a single *POT1* gene, whereas 2 *Pot1* genes exist in the mouse genome. Although both Pot1 proteins display a high degree of sequence conservation and form heterodimers with the shelterin component TPP1, knockout mouse models reveal that Pot1a and Pot1b display divergent functions. The Pot1a-TPP1 complex primarily mediates telomere end protection by repressing the activation of an ATR-dependent DNA damage checkpoint via the exclusion of RPA binding to single-stranded telomeric DNA.[25,47,48] This complex is also required to repress the alternative-nonhomologous end joining DNA repair pathway at telomeres.[49] The Pot1b-TPP1 complex is also involved in repressing the ATR-dependent DNA damage pathway at chromosome ends.[20] However, the major function of Pot1b appears to be its role in protecting the C-rich telomeric DNA from nucleolytic processing. Deletion of *Pot1b* results in the formation of very long G-rich overhangs because of unrestrained nucleolytic processing of the 5′ end of the C-rich strand by as yet unknown nucleases, with progressive loss of total telomere length.[19,20] The elongated overhang could serve as a substrate for the recruitment of RPA, resulting in the activation of an ATR-p53–dependent checkpoint response to compromise HSC function. Given the high degree of sequence conservation present in all POT1 genes, and the observation that the human POT1 protein possess functions found in both Pot1a and Pot1b,[50] analysis of patients with BM failure syndromes should include genetic analysis of the POT1 gene.

Acknowledgments

The authors thank Dr James You, Department of Hematopathology, MD Anderson Cancer Center, for helping us acquire several BM photomicrographs and Jan Karlseder, Salk Institute, for providing antimouse TRF1 antibody. S.C. acknowledges technical support from Dr Asha Multani of the MDACC cytogentics core facility.

S.C. is grateful for financial support from the Department of Laboratory Medicine, Yale University School of Medicine and the National Cancer Institute (RO1 CA129037).

Authorship

Contribution: Y.W. designed and performed the experiments, helped write the paper, and created the figures; M.-F.S. maintained mouse colonies; and S.C. analyzed and interpreted the data, wrote the paper, and finalized the figures.

Conflict-of-interest disclosure: The authors declare no competing financial interests.

Correspondence: Sandy Chang, Department of Laboratory Medicine, Yale University School of Medicine, 330 Cedar Street, New Haven, CT 06520; e-mail: s.chang@yale.edu.

References

1. Hoeijmakers JHJ. DNA damage, aging, and cancer. *N Engl J Med.* 2009;361(15):1475-1485.
2. Greider CW. Telomere length regulation. *Annu Rev Biochem.* 1996;65:337-365.
3. Bodnar AG, Ouellette M, Frolkis M, et al. Extension of life-span by introduction of telomerase into normal human cells. *Science.* 1998;279(5349):349-352.
4. Vaziri H, Dragowska W, Allsopp RC, et al. Evidence for a mitotic clock in human hematopoietic stem cells: loss of telomeric DNA with age. *Proc Natl Acad Sci U S A.* 1994;91(21):9857-9860.
5. Rufer N, Dragowska W, Thornbury G, et al. Telomere length dynamics in human lymphocyte subpopulations measured by flow cytometry. *Nat Biotechnol.* 1998;16(8):743-747.
6. Vulliamy T, Marrone A, Goldman F, et al. The RNA component of telomerase is mutated in autosomal dominant dyskeratosis congenita. *Nature.* 2001;413(6854):432-435.
7. Marrone A, Walne A, Tamary H, et al. Telomerase reverse-transcriptase homozygous mutations in autosomal recessive dyskeratosis congenita and Hoyeraal-Hreidarsson syndrome. *Blood.* 2007;110(13):4198-4205.
8. Vulliamy T, Marrone A, Szydlo R, et al. Disease anticipation is associated with progressive telomere shortening in families with dyskeratosis congenita due to mutations in TERC. *Nat Genet.* 2004;36(5):447-449.
9. Armanios M, Chen JL, Chang YP, et al. Haploinsufficiency of telomerase reverse transcriptase leads to anticipation in autosomal dominant dyskeratosis congenita. *Proc Natl Acad Sci U S A.* 2005;102(44):15960-15964.
10. Cawthon RM, Smith KR, O'Brien E, et al. Association between telomere length in blood and mortality in people aged 60 years or older. *Lancet.* 2003;361(9355):393-395.
11. Blasco MA, Lee HW, Hande MP, et al. Telomere shortening and tumor formation by mouse cells lacking telomerase RNA. *Cell.* 1997;91(1):25-34.
12. Lee HW, Blasco MA, Gottlieb GJ, et al. Essential role of mouse telomerase in highly proliferative organs. *Nature.* 1998;392(6676):569-574.
13. Samper E, Flores JM, Blasco MA. Restoration of telomerase activity rescues chromosomal instability and premature aging in Terc−/− mice with short telomeres. *EMBO Rep.* 2001;2(9):800-807.
14. Jaskelioff M, Muller FL, Paik JH, et al. Telomerase reactivation reverses tissue degeneration in aged telomerase-deficient mice. *Nature.* 2011;469(7328):102-106.
15. Chan SS, Chang S. Defending the end zone: studying the players involved in protecting chromosome ends. *FEBS Lett.* 2010;584(17):3773-3778.
16. Hockemeyer D, Daniels J-P, Takai H, et al. Recent expansion of the telomeric complex in rodents: two distinct POT1 proteins protect mouse telomeres. *Cell.* 2006;126(1):63-77.
17. He H, Multani AS, Cosme-Blanco W, et al. POT1b protects telomeres from end-to-end chromosomal fusions and aberrant homologous recombination. *EMBO J.* 2006;25(21):5180-5190.
18. Wu L, Multani AS, He H, et al. Pot1 deficiency initiates DNA damage checkpoint activation and aberrant homologous recombination at telomeres. *Cell.* 2006;126(1):49-62.
19. Hockemeyer D, Palm W, Wang RC, et al. Engineered telomere degradation models dyskeratosis congenita. *Genes Dev.* 2008;22(13):1773-1785.
20. He H, Wang Y, Guo X, et al. Pot1b deletion and telomerase haploinsufficiency in mice initiate an ATR-dependent DNA damage response and elicit phenotypes resembling dyskeratosis congenita. *Mol Cell Biol.* 2009;29(1):229-240.
21. Savage SA, Giri N, Baerlocher GM, et al. TINF2, a component of the shelterin telomere protection complex, is mutated in dyskeratosis congenita. *Am J Human Genet.* 2008;82(2):501-509.
22. Walne AJ, Vulliamy T, Beswick R, et al. TINF2 mutations result in very short telomeres: analysis of a large cohort of patients with dyskeratosis congenita and related bone marrow failure syndromes. *Blood.* 2008;112(9):3594-3600.
23. Liu G, Parant JM, Lang G, et al. Chromosome stability, in the absence of apoptosis, is critical for suppression of tumorigenesis in Trp53 mutant mice. *Nat Genet.* 2004;36(1):63-68.
24. Hawkins AL, Jones RJ, Zehnbauer BA, et al. Fluorescence in situ hybridization to determine engraftment status after murine bone marrow transplant. *Cancer Genet Cytogenet.* 1992;64(2):145-148.
25. Guo X, Deng Y, Lin Y, et al. Dysfunctional telomeres activate an ATM-ATR-dependent DNA damage response to suppress tumorigenesis. *EMBO J.* 2007;26(22):4709-4719.
26. Essers MA, Offner S, BlancoBose WE, et al. IFNalpha activates dormant haematopoietic stem cells in vivo. *Nature.* 2009;458(7240):904-908.
27. Randall TD, Weissman IL. Phenotypic and functional changes induced at the clonal level in hematopoietic stem cells after 5-fluorouracil treatment. *Blood.* 1997;89(10):3596-3606.
28. Deng Y, Chan SS, Chang S. Telomere dysfunction and tumour suppression: the senescence connection. *Nat Rev Cancer.* 2008;8(6):450-458.
29. Rudolph KL, Chang S, Lee H-W, et al. Longevity, stress response, and cancer in aging telomerase-deficient mice. *Cell.* 1999;96(5):701-712.
30. Cosme-Blanco W, Shen MF, Lazar AJ, et al. Telomere dysfunction suppresses spontaneous tumorigenesis in vivo by initiating p53-dependent cellular senescence. *EMBO Rep.* 2007;8(5):497-503.

31. Takai H, Smogorzewska A, de Lange T. DNA damage foci at dysfunctional telomeres. *Curr Biol.* 2003;13(17):1549-1556.
32. d'Adda di Fagagna F, Reaper PM, Clay-Farrace L, et al. A DNA damage checkpoint response in telomere-initiated senescence. *Nature.* 2003;426(6963): 194-198.
33. Brown JP, Wei W, Sedivy JM. Bypass of senescence after disruption of p21CIP1/WAF1 gene in normal diploid human fibroblasts. *Science.* 1997; 277(5327):831-834.
34. Itahana K, Dimri G, Campisi J. Regulation of cellular senescence by p53. *Eur J Biochem.* 2001; 268(10):2784-2791.
35. Beauséjour CM, Krtolica A, Galimi F, et al. Reversal of human cellular senescence: roles of the p53 and p16 pathways. *EMBO J.* 2003;22(16): 4212-4222.
36. Hills M, Lansdorp PM. Short telomeres resulting from heritable mutations in the telomerase reverse transcriptase gene predispose for a variety of malignancies. *Ann N Y Acad Sci.* 2009;1176: 178-190.
37. Ohyashiki JH, Iwama H, Yahata N, et al. Telomere stability is frequently impaired in high-risk groups of patients with myelodysplastic syndromes. *Clin Cancer Res.* 1999;5(5):1155-1160.
38. Calado RT, Regal JA, Hills M, et al. Constitutional hypomorphic telomerase mutations in patients with acute myeloid leukemia. *Proc Natl Acad Sci U S A.* 2009;106(4):1187-1192.
39. Kirwan M, Vulliamy T, Marrone A, et al. Defining the pathogenic role of telomerase mutations in myelodysplastic syndrome and acute myeloid leukemia. *Hum Mutat.* 2009;30(11):1567-1573.
40. Calado RT, Young NS. Telomere maintenance and human bone marrow failure. *Blood.* 2008; 111(9):4446-4455.
41. Brümmendorf TH, Maciejewski JP, Mak J, et al. Telomere length in leukocyte subpopulations of patients with aplastic anemia. *Blood.* 2001;97(4): 895-900.
42. Wang F, Podell ER, Zaug AJ, et al. The POT1-TPP1 telomere complex is a telomerase processivity factor. *Nature.* 2007;445(7127):506-510.
43. Xin H, Liu D, Wan M, et al. TPP1 is a homologue of ciliate TEBP-beta and interacts with POT1 to recruit telomerase. *Nature.* 2007;445(7127):559-562.
44. Yang D, He Q, Kim H, et al. TIN2 dyskeratosis congenital missense mutants are defective in association with telomerase. *J Biol Chem.* 2011; 286(26):23022-23030.
45. Abreu E, Aritonovska E, Reichenbach P, et al. TIN2-tethered TPP1 recruits human telomerase to telomeres in vivo. *Mol Cell Biol.* 2010;30(12): 2971-2982.
46. Rossi DJ, Bryder D, Seita J, et al. Deficiencies in DNA damage repair limit the function of haematopoietic stem cells with age. *Nature.* 2007; 447(7145):725-729.
47. Denchi EL, de Lange T. Protection of telomeres through independent control of ATM and ATR by TRF2 and POT1. *Nature.* 2007;448(7157):1068-1071.
48. Flynn RL, Centore RC, O'Sullivan RJ, et al. TERRA and hnRNPA1 orchestrate an RPA-to-POT1 switch on telomeric single-stranded DNA. *Nature.* 2011;471(7339):532-536.
49. Rai R, Zheng H, He H, et al. The function of classical and alternative non-homologous end-joining pathways in the fusion of dysfunctional telomeres. *EMBO J.* 2010;29(15):2598-2610.
50. Palm W, Hockemeyer D, Kibe T, et al. Functional dissection of human and mouse POT1 proteins. *Mol Cell Biol.* 2009;29(2):471-482.